Magnetic Resonance Imaging 44 (2017) 8–14

Contents lists available at ScienceDirect

Magnetic Resonance Imaging

journal homepage: www.mrijournal.com

Original contribution

Assessment of MRI issues for a new cerebral spinal fluid shunt, gravitational valve (GV)

Daniel Moghtader [a], Hans-Joachim Crawack [b], Christoph Miethke [b], Zinah Dörlemann [b], Frank G. Shellock [c,d,*]

[a] Department of Chemistry and Biochemistry, Loyola Marymount University, 1 Loyola Marymount University Dr., Los Angeles, CA 90045, United States
[b] Christoph Miethke GmBH & Co. KG, Ulanenweg 2, D-14469 Potsdam, Germany
[c] Department of Radiology, Keck School of Medicine, University of Southern California, 7751 Veragua Dr., Playa Del Rey, CA 90293, United States
[d] Department of Medicine, Keck School of Medicine, University of Southern California, 7751 Veragua Dr., Playa Del Rey, CA 90293, United States

ARTICLE INFO

Article history:
Received 19 May 2017
Accepted 13 July 2017

Keywords:
Gravititational valve
Cerebral spinal fluid
American Society for Testing and Materials International
Specific absorption rate
MRI Safety

ABSTRACT

Purpose: A gravitational valve (GV) may be used to treat hydrocephalus, offering possible advantages that include avoidance of over drainage and long-term complications. Because a GV is made from metal, there are potential safety and other problems related to the use of MRI. The objective of this investigation was to evaluate MRI-related issues (i.e., magnetic field interactions, heating, and artifacts) for a newly developed, metallic GV.
Methods: Tests were performed on the GV (GAV 2.0) using well-accepted techniques to assess magnetic field interactions (translational attraction and torque, 3-Tesla), MRI-related heating (1.5-T/64-MH and 3-T/128-MHz, whole body averaged SAR, 2.7-W/kg and 2.9-W/kg, respectively), artifacts (3-Tesla; gradient echo and T1-weighted, spin echo sequences), and possible functional changes related to exposures to different MRI conditions (exposing six samples each to eight different pulse sequences at 1.5-T/64-MHz and 3-T/128-MHz).
Results: Magnetic field interactions were not substantial (deflection angle 2°, no torque) and heating was minor (highest temperature rise, ≥1.9 °C, highest background temperature rise, ≥1.7 °C). Artifacts on the gradient echo pulse sequence extended approximately 10 mm from the size and shape of the GV. The different exposures to 1.5-T/64-MHz and 3-T/128-MHz conditions did not alter or damage the operational aspects of the GV samples.
Conclusions: The findings demonstrated that MRI can be safely used in patients with this GV and, thus, this metallic implant is deemed acceptable or "MR Conditional" (i.e., using current labeling terminology), according to the conditions used in this study.

1. Introduction

Currently, the implantation of cerebral spinal fluid (CSF) shunt is the most frequently used therapy for hydrocephalus [1]. The clinical picture of hydrocephalus comprises a disturbed balance between CSF production and resorption caused by various reasons, including obstructions between the different CSF-filled compartments and pathologic CSF production [1]. As a result, this imbalance leads to an overpressure in the ventricles.

The implantation of a shunt serves to drain excess CSF from the ventricles of the brain to other body compartments, such as the peritoneal cavity, that are suited for resorption [1,2]. The shunt is implanted subcutaneously and essentially consists of at least one differential pressure valve (DPV) or unit, a reservoir for CSF extraction and fluid control, and various flexible silicone catheters [1,2]. The DPV is technically characterized by its opening pressure and serves to keep the intraventricular pressure on a defined physiological level, to regulate the CSF flow rate, and the flow direction [3]. Additionally, an anti-siphon device, such as a gravitational unit, is part of the shunt, which prevents the dangerous over drainage when the patient is in a standing position [4–7].

Many different types of shunt devices exist which differ in size, functional principal, operational features, and in materials [3]. In addition to a simple DPV that has a fixed opening pressure, there is also a "programmable valve" in which the opening pressure can be adjusted non-invasively by means of magnetic forces using an externally applied programmer. In all cases, the shunt valve type and the required opening pressure are carefully selected by an experienced neurosurgeon depending on the individual needs of the patient.

Nearly all modern-day valves contain para- and/or ferromagnetic material or, in case of programmable (i.e., adjustable) valves, small magnets that are able to interact with an externally applied magnetic field.

For some types of programmable valves that incorporate magnets, it is well known that relatively weak external magnetic fields (e.g., toy-

* Corresponding author at: University of Southern California, 7751 Veragua Dr., Playa Del Rey, CA 90293, United States.
E-mail addresses: hansjoachim.crawack@miethke.com (H.-J. Crawack), Christoph.miethke@miethke.com (C. Miethke), Zinah.Doerlemann@miethke.com (Z. Dörlemann), frank.shellock@mrisafety.com (F.G. Shellock).

http://dx.doi.org/10.1016/j.mri.2017.07.018
0730-725X/

related magnets or those in headphones) can unintentionally change their opening pressure settings and, in certain cases, the function of the valve can be damaged [3,8–14]. Not surprisingly, the power static magnetic fields used by clinical magnetic resonance imaging (MRI) systems may create deleterious effects on these programmable valves and, as such, patients that present with these implants must be identified during the screening process in order to ensure their safety relative to the use of MRI technology [15–17]. For example, magnetic field interactions, exerting translational attraction and torque, could move or rotate the implanted programmable shunt valve and/or act on the movable, internal parts and adversely affect its function. In some cases, the small magnets inside of programmable CSF shunt valves can either be permanently damaged or have reversed polarity related to exposure to the powerful static magnetic fields associated with MRI systems. Other potential issues also exist including MRI-related heating of the metallic components and the substantial signal loss and distortion artifacts caused by the high magnetic susceptibility associated with the small magnets of the programmable valve [17]. The latter problem may pose special risks for the patient because the diagnostically critical details can be diminished or completely obliterated on the MR images [15,16].

A gravitational valve (GV) is a viable alternative to the use of a simple programmable valve for certain patients [1,5–7]. Basically, a GV consists of two valves in one housing - one is posture-independent and the other is sensitive to the patient's postural changes. Recently, a new GV (GAV 2.0) was developed that is made from metallic materials. Considering the afore-mentioned concerns associated with MRI, the objective of this investigation was to evaluate magnetic field interactions (translational attraction and torque), MRI-related heating, artifacts, and possible functional changes for this neurological implant.

2. Materials and methods

2.1. Gravitational valve

A newly developed, gravitational valve (GV) (GAV 2.0, Miethke GmbH & Co. KG, Potsdam, Germany, www.miethke.com) underwent MRI testing in this investigation. This unique GV is primarily a combination of a differential pressure unit (i.e., ball-in-cone technology with a fixed opening pressure) and a gravitational unit (i.e., ball-in-cone technology responding to positional changes, variable opening pressure) whose function depends on its inclination angle, thus, allowing it to respond to the patient's postural changes (Fig. 1a and b). The gravitational unit functions as an "anti-siphon-device" for effective protection and prevention against over drainage when the patient is in a standing position. The GV also has a pressure coding segment in which different geometrical forms are located that can easily be recognized and distinguished on X-ray, and are specific to a given opening pressure combination for the patient's lying and upright postures (Fig. 2a and b). All components are integrated in a single tubular housing made from titanium alloy (TiAl6V4).

From an operational consideration, with the GV in the "lying" position (Fig. 2a), the tantalum ball is positioned such that there is no impact on the other parts. The overall opening pressure is only determined by the differential pressure unit with the GV in this position. In the "upright" position (Fig. 3), the mobile tantalum ball pushes another sapphire ball, effectively increasing the opening pressure as the gravitational unit is activated, automatically adjusting the opening pressure according to the patient's posture.

2.2. MRI systems

For the MRI tests performed on the GV, the following MRI systems were used: 1.5-Tesla/64-MHz (Magnetom, software version Numaris/4, Version Syngo MR 2002B DHHS, Siemens Medical Solutions, Malvern, PA) and 3-T/128-MHz MR system (Excite HDx, software version 14×.M5, GE Healthcare, Milwaukee, WI).

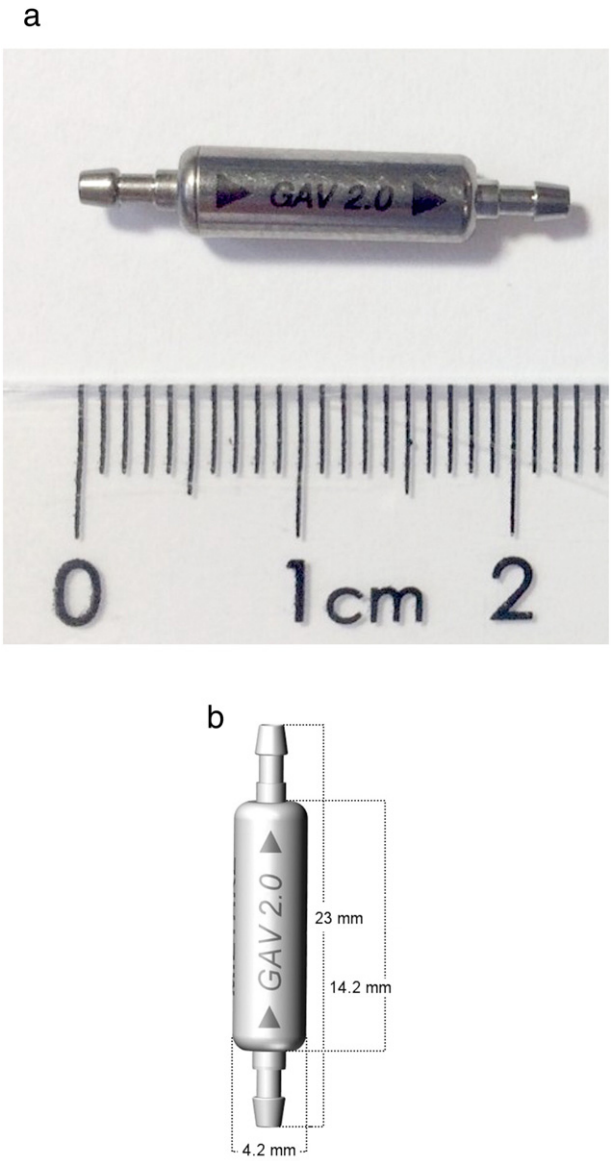

Fig. 1. a. Photograph of the GV (GAV 2.0) that underwent MRI testing. b. Basic diagram showing the GV (GAV 2.0). Note the dimensions of this implant.

2.3. Magnetic field interactions

Testing for magnetic field interactions involved assessments of translational attraction and torque for the GV at 3-Tesla.

2.3.1. Translational attraction

The deflection angle measurement technique was used to determine translational attraction for the GV, as previously described [18–21]. Using this method, the GV was suspended from a 20-cm length of light-weight string (<10% of the weight of the implant) that was attached at the 0-degree position on a protractor that was fixed on a test apparatus [18–21]. The test apparatus was positioned in the MR system at the point of the highest "patient accessible" spatial gradient magnetic field [22] which was 466-gauss/cm, as determined using a gauss meter (Extech 480,823 Electromagnetic Field and Extremely Low Frequency Meter; Extech, Nashua, NH). The deflection angle from

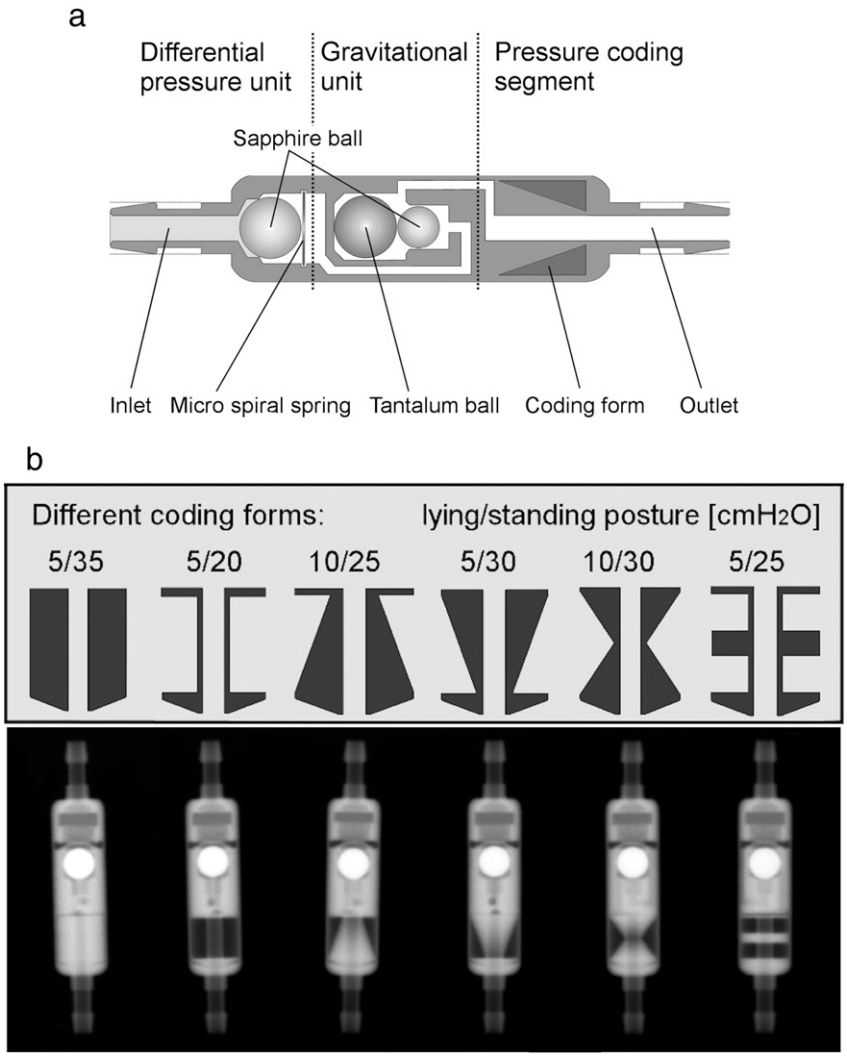

Fig. 2. a. Detailed schematic of the GV (GAV 2.0). Note the various parts including the differential pressure unit, gravitational unit, and the pressure coding segment. The internal components include a micro-spiral spring, two sapphire balls, one tantalum ball (which is heavier than the sapphire balls), and the coding form that varies according to an opening pressure combination for the patient's lying and upright postures. Also, note the positions of the internal components as they would be oriented with the patient in a lying position. b. The different geometrical forms located in the pressure coding segment of the GV (top) that can easily be recognized and distinguished on x-ray (bottom). Each coding form varies according to an opening pressure combination for the patient's lying and upright postures.

the vertical position to the nearest 1-degree was measured three times and a mean value was calculated [18–21].

2.3.2. Torque

Magnetic-field induced torque was evaluated for the GV using a previously described technique [18–21]. The test consisted of placing the GV along its long axis on a near-frictionless, flat plastic plate with millimeter markings at a 45-degree orientation relative to the direction (i.e., horizontal) MR system's static magnetic field [18–21]. The plate with the GV was then placed at the center of the scanner, where the effect of torque acting on metallic object is known to predominate [17–21]. Rotation (i.e., alignment) of the GV to the static magnetic field was carefully observed with the investigator inside of the bore of the MR system. This procedure was repeated to encompass a full 360-degrees of rotation for the GV. Torque was characterized for the GV, according to the following scale [18–21]: 0, no torque; +1: mild or low torque, the implant moved slightly but did not align to the magnetic field; +2: moderate torque, the occlusion balloon eventually aligned to the magnetic field; +3: strong torque, the occlusion balloon aligned rapidly to the magnetic field; +4: very strong torque, the implant shows very rapid and forceful alignment to the magnetic field.

2.4. MRI-related heating

Because MRI-related heating for a metallic implant is different depending on the transmitted RF frequency [17], the GV underwent evaluation at both 1.5-T/64-MHz and a 3-T/128-MHz in accordance with the recommendations of the American Society of Testing and Materials (ASTM) International and based on prior reports [18–20,23,24]. The GV was placed into the ASTM International phantom that was filled to a depth of 10 cm with gelled saline (0.8 g/L NaCl plus 5.85 g/L polacrylic acid in distilled water) [18–20,23,24]. Notably, the GV was in a position within the phantom that would result in possible substantial MRI-related heating because of the high, uniform electric field that exists tangential to the implant. This ensured extreme radiofrequency heating conditions for this experimental setup that was based on an analysis of the ASTM International phantom and the MRI conditions used for this assessment [18–20,23,24]. Temperature measurements were obtained using a fluoroptic thermometry system (Model 3100, LumaSense Technologies, Santa Clara, CA) with temperature probes placed on either end and in the middle of the GV [18–20,23,24].

MRI was conducted at 1.5-Tesla/64-MHz and 3-T/128-MHz using the transmit body radiofrequency (RF) coil and parameters that would

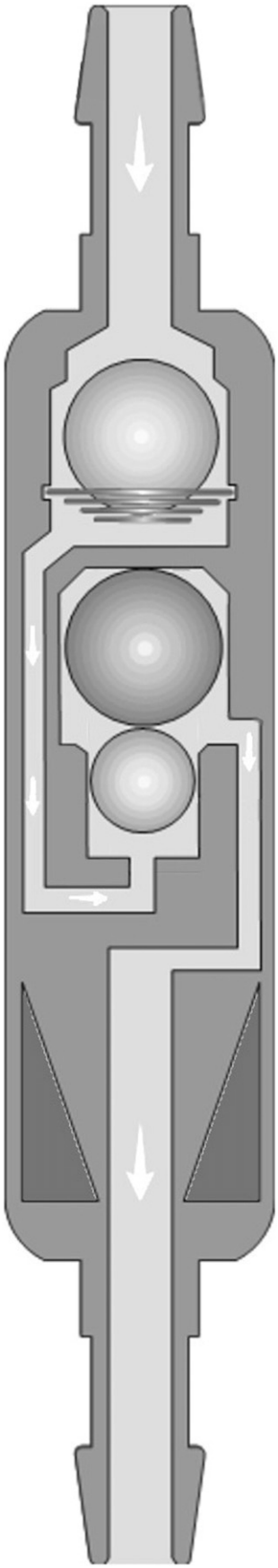

Fig. 3. With the patient in a standing position (i.e., "upright" position for the GV), the tantalum ball within the gravitational unit moves against the sapphire ball, increasing the effective opening pressure, thus, counteracting the related high hydrostatic suction, creating an anti-siphoning effect.

generate a relatively high MR system-reported, whole body averaged specific absorption rate (SAR) in each case (1.5-T/64-MHz, whole body average SAR, 2.7-W/kg; 3-T/128-MHz, whole body average SAR, 2.9-W/kg) for a total imaging time of 15 min [18–24]. The landmarking position (i.e., the center position or anatomic region for MRI) and section locations were selected to encompass the entire area of the GV.

2.4.1. Experimental protocol

The GV was positioned in the phantom, as previously-described. The fluoroptic thermometry system was calibrated and the fluoroptic thermometry probes were applied to the implant. The head/torso phantom was filled with the gelled-saline and allowed to equilibrate to the environmental temperature for >24 h, in each MRI environment (i.e., 1.5-T/64-MHz and 3-T/128-MHz). The room and MR system bore temperatures were at constant levels throughout the experimental sessions. After recording baseline temperatures (5 min), MRI was conducted for 15 min with temperatures recorded at 5-s intervals. The MRI-related heating tests were performed on separate days at 1.5-Tesla/64-MHz and 3-Tesla/128-MHz. The highest temperature changes recorded by the fluoroptic thermometry probes are reported for the GV for each MRI condition.

In addition, background temperatures (i.e., without the GV present in the phantom) were recorded in the gelled-saline-filled ASTM International phantom my measuring temperatures under the same conditions with the temperature probes positioned in the same positions as those used with the GV present in the phantom [18–20,23,24].

2.5. Assessment of artifacts

Artifacts were assessed for the GV at 3-Tesla according to a previously-described protocol [18–20,24]. MRI was performed with the implant attached to a plastic frame that was placed inside of the gadolinium-doped, saline-filled, plastic phantom. A transmit send/receive RF head coil (i.e., for increased signal-to-noise) and the following pulse sequences were used: T1-weighted, spin echo; repetition time, 500 msec; echo time, 20 msec; matrix size, 256 × 256; section thickness, 5 mm; field of view, 24 cm; number of excitations, 2; bandwidth; 16 kHz; and gradient echo pulse sequence (GRE); repetition time, 100 msec; echo time, 15 msec; flip angle 30°; matrix size, 256 × 256; section thickness, 5 mm; field of view, 24 cm; number of excitations, 2; bandwidth, 16 kHz [18–20,24]. The imaging planes were positioned to include the long and short axes of the GV and selected image locations were obtained through the implant after inspection of multiple "scout" MR images to represent the largest or worst-case artifact size. This ensured that the sizes of the artifacts were not underestimated. The image display parameters (i.e., window and level settings, magnification, etc.) were selected and applied in a consistent manner to ensure accurate measurements. Planimetry software provided with the MR system was utilized to measure (accuracy and resolution ± 10%) the cross-sectional areas of the largest artifact size for the GV, for each pulse sequence and imaging plane associated [18–20,24]. This well-accepted methodology of characterizing artifacts has been applied in previous investigations, and thus, provides an acceptable means of comparison to other implants [18–20,24].

2.6. Assessment of exposures to 1.5-Tesla/64-MHz and 3-Tesla/128-MHz MRI conditions

To determine if the GV sustains a change in function or is damaged, experiments were performed to assess the effects of exposing multiple samples of this implant to 1.5-Tesla/64-MHz and 3-Tesla/128-MHz MRI conditions, according to a previously methodology [18–20,24]. A total of 12 samples of the GV underwent comprehensive evaluations involving a range of tests that were designed and performed by the manufacturer (Miethke GmbH & Co. KG, Potsdam, Germany) to characterize

the functional aspects of these implants before and after exposing them to the MRI conditions. Six different samples of the GV oriented in orthogonal planes (2, axial; 2 sagittal; 2, coronal) were subjected to eight different pulse sequences selected to be representative of typical clinical imaging techniques in order to cover a range of possible scenarios with regard to having a patient with this implant undergoing MRI at 1.5-Tesla/64-MHz or 3-Tesla/128-MR systems (Table 1) [18–20,24].

The samples of the GV were attached to a fluid-filled, cylinder-shaped phantom using porous paper tape (i.e., two samples each positioned in each of the three orthogonal orientations). The cylinder-shaped phantom with the samples was then placed into a larger plastic phantom (length, 40 cm; width, 30 cm; height, 22 cm) filled with approximately 5 l of normal saline to provide a conductive medium around the implants and to "load" the transmit/receive RF body coil for each respective MR system [18–20,24].

After performing the pre-MRI functional test procedures, MRI was then conducted on the cylinder-shaped phantom with the six different samples of the GV after it was placed inside of the water-filled box-shaped phantom using the 1.5-Tesla/64-MHz and 3-Tesla/128-MHz MR systems. The land-marking position (i.e., the center position or anatomic region for the MRI) and multiple section locations were selected to encompass every GV sample to ensure thorough and complete exposures to the MRI conditions. After the respective exposures, each GV was carefully removed, returned to the manufacturer, and post-MRI functional testing was conducted.

3. Results

The mean deflection angle for the GV was $2 \pm 0°$ and the torque was 0, no torque. The highest temperature rise for the GV at 1.5-Tesla/64-MHz was 1.6 °C (highest background temperature rise, 1.4 °C) and at 3-Tesla/128-MHz it was 1.9 °C (highest background temperature rise, 1.7 °C).

The artifact size results for the GV are presented in Table 2. Artifacts appeared as low signal intensity signal voids that were relatively small in relation to the size and shape of the GV, with no apparent distortion seen on the MR images. The GRE pulse sequence produced larger artifacts than the T1-weighted, spin echo pulse sequence. The greatest amount of signal loss extended approximately 10 mm in relation to the size and shape of this implant as seen on the GRE sequence. Fig. 4a and b show examples of the artifacts for the GV.

Based on the tests performed to characterize the functional aspects of the GV, there was no evidence of a change in function or damage for test sample in association with exposures to the 1.5-Tesla/64-MHz and 3-Tesla/128-MHz MRI conditions. Thus, the function of each GV sample was preserved, especially the characteristic opening pressure value associated with a "lying" versus an "upright" position.

4. Discussion

The particular GV (GAV 2.0) that underwent MRI testing is an improved type of shunt implant because it was specially developed for both adult and pediatric applications, as well as for other reasons. For example, an important feature of this GV is a design that optimizes the CSF flow path, which may diminish the possibility of occlusion. Additionally, the size of this GV (i.e., 4.2-mm width × 23-mm length) is critical because it is intended to minimize or prevent irritation and/or rupture of delicate skin, especially when implanted in newborns and infants. This GV integrates several characteristic coding geometries that facilitate the distinction of the different opening pressure combinations as seen on x-ray (Fig. 2b). Thus, confusion regarding the particular GV version (i.e., a certain geometric form is associated with a certain opening pressure combination) that is present in the patient is effectively avoided. According to an analysis of the patient's clinical needs, a full range of pressure-stage-combination are provided by the different versions of this GV (i.e., lying/upright posture - 5/35 cmH_2O, 5/20 cmH_2O, 10/25 cmH_2O, 5/30 cmH_2O,10/30 cmH_2O, and 5/25 cmH_2O) The gravitational unit integrated in the GV serves to compensate for the high hydrostatic suction that, according to the laws of physics, is always and unavoidably present when the patient is in a standing position. Because this GV is made from metallic materials, possible risks exist for the patient related to MRI [17].

4.1. MRI test findings

The deflection angle measured for the GV was 2° and there was no torque exhibited by this implant. According to ASTM International [21], "…if an implant deflects less than 45°, then the magnetically induced force is less than the weight of the implant." Therefore, GV is well within the acceptable criterion for translational attraction for this implant. Thus, from a magnetic field interaction consideration, this implant poses no risk to a patient undergoing MRI at 3-Tesla or less.

Table 1
Parameters used to expose the GV (six samples each) to 1.5-Tesla/64-MHz and 3-Tesla/128-MHz MRI conditions.

1.5-Tesla/64-MHz MRI conditions								
Pulse Sequence	#1	#2	#3	#4	#5	#6	#7	#8
	T1-SE	T2-SE	T1-FSE	T2-FSE	GRE, 3D	FGRE, 3D	GRE, MTC	EPI
TR (msec.)	700	3000	700	5000	20	3.7	628	3400
TE (msec.)	10	100	12	113	3	1.1	10	103
Flip angle	N/A	N/A	N/A	N/A	25	8	5	N/A
Field of view	30 cm	30 cm	30 cm	30 cm	30 cm	30 cm	30 cm	30 cm
Section thick	10 mm	10 mm	10 mm	10 mm	3 mm	3 mm	10 mm	1 mm
Imaging plane	Axial	Axial	Axial	Axial	Volume	Volume	Axial	Axial
3-Tesla/128-MHz MRI conditions								
Pulse Sequence	#1	#2	#3	#4	#5	#6	#7	#8
	T1-SE	T2-SE	T1-FSE	T2-FSE	GRE, 3D	FGRE, 3D	GRE, MTC	EPI
TR (msec.)	700	3000	700	5000	20	3.7	628	3400
TE (msec.)	10	100	12	113	3	1.1	10	103
Flip angle	N/A	N/A	N/A	N/A	25	8	5	N/A
Field of view	30 cm	30 cm	30 cm	30 cm	30 cm	30 cm	30 cm	30 cm
Section thick	10 mm	10 mm	10 mm	10 mm	3 mm	3 mm	10 mm	1 mm
Imaging plane	Axial	Axial	Axial	Axial	Volume	Volume	Axial	Axial

(T1-SE, T1-weighted spin echo; T2-SE, T2-weighted spin echo; T1-FSE, T1-weighted fast spin echo; T2-FSE, T2-weighted fast spin echo; GRE, gradient echo; 3D, three-dimensional; FGRE, fast gradient echo; MTC, magnetization transfer contrast; EPI, echo planar imaging; N/A, not applicable; GRE, gradient echo; SE, spin echo; SAR, specific absorption rate).

Table 2
Artifact size at 3-Tesla for the GV.

Pulse sequence	Area (mm^2)	Imaging plane
T1-spin, echo	455	Long axis
T1-spin, echo	300	Short axis
GRE	799	Long axis
GRE	768	Short axis

Excessive temperature rises may be generated in metallic implants during MRI, resulting in patient injuries [17]. MRI-related heating performed at relatively high, MR system reported SAR levels at 1.5-Tesla/64-MHz (whole body averaged SAR, 2.7-W/kg) and 3-Tesla/128-MHz (whole body averaged SAR, 2.9-W/kg) was relatively minor for the GV (i.e., highest temperature rise, ≥1.9 °C, highest background temperature rise, ≥1.7 °C). Thus, these findings demonstrated that heating is not concern for this metallic implant.

Artifacts extended approximately 10 mm in relation to the size and shape of the GV as seen on the GRE sequence at 3-Tesla, such that anatomy located at a position greater than this distance may be visualized on MRI (i.e., in association with comparable imaging parameters).

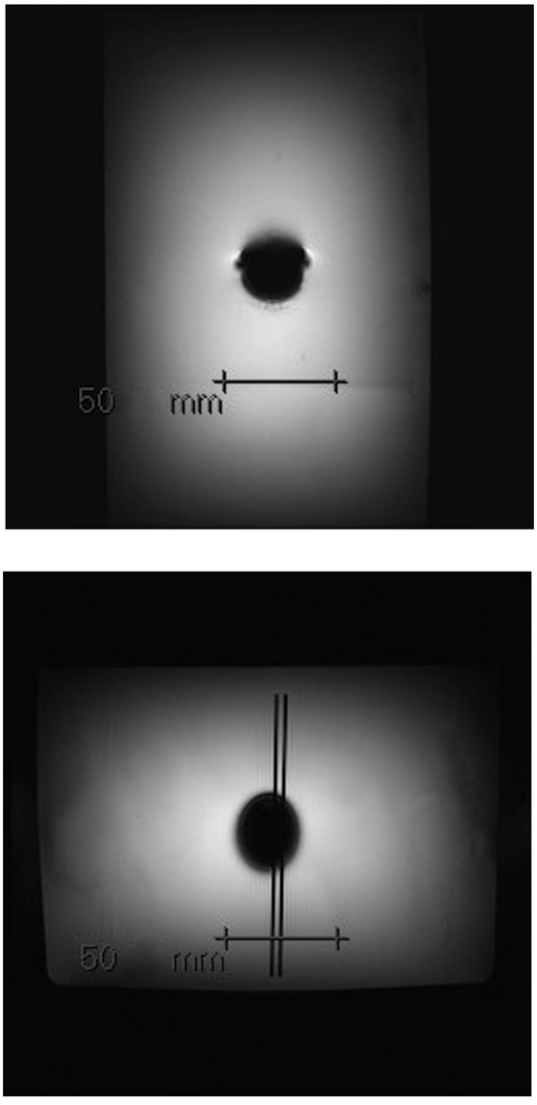

Fig. 4. MR images showing artifacts at 3-Tesla for the GV on gradient echo pulse sequence. a, Section location oriented to the long-axis of the GV. b, Section location oriented to the short axis of the GV (note the line corresponding to the plastic frame to which the GV was attached).

Given the importance of maintaining the diagnostic integrity of MRI, consideration should be given to reducing the size of the artifact when this GV is implanted in or near the area of interest by selecting imaging parameters that are optimized (e.g., use a fast spin echo pulse sequence, increase the read-out bandwidth, increase the matrix size, decrease the voxel size, etc.) or by implementing MR system-based, metal reduction software (e.g., metal artifact reduction sequence, MARS, or slice encoding for metal artifact correction with view angle tilting, SEMAC-VAT).

A malfunctioning or damaged GV can cause serious problems for the patient due to over drainage and/or elevated intracranial pressure. Therefore, it is essential to identify possible functional alterations that could potentially occur with this implant in association with MRI. Fortunately, the different exposures to 1.5-T/64-MHz and 3-T/128-MHz conditions did not alter or damage the operational aspects of the GV samples. This is not surprising considering that the primary materials (titanium alloy, tantalum, sapphire) comprising this implant have relatively low magnetic susceptibility values. Importantly, unlike magnetically-programmable, CSF shunt valves, the function of this GV (GAV 2.0) will not be impacted by the electromagnetic fields used for MRI.

5. Conclusions

MRI testing performed on the GV demonstrated that this implant is acceptable or, using current MRI labeling terminology [25], "MR Conditional" (i.e., an item that has been demonstrated to pose no known hazards in a specified MR environment with specified conditions of use) at 1.5-T/64-MHz and 3-T/128-MHz. This information is noteworthy when screening a patient with this metallic implant device because there is no reason to withhold MRI from patients that have this shunt device.

References

[1] Miethke C. Shunt and valve technology. In: Fritsch M, Kehler U, Meier U, editors. Chapter 9. Normal pressure hydrocephalus: pathophysiology diagnosis treatment. New York, Delhi, Rio: Thieme Stuttgart; 2014. p. 57–83.
[2] Miethke C. Chapter 5: manufacture and function of cerebrospinal fluid shunts. In: Kombogiorgas D, editor. The cerebrospinal fluid shunts. New York: Nova Science; 2016. p. 99–220.
[3] Chari A, Czosnyka M, Richards HK, et al. Hydrocephalus shunt technology: 20 years of experience from the Cambridge Shunt Evaluation Laboratory. J Neurosurg 2014; 120:697–707.
[4] Freimann FB, Kimura T, Stockhammer F, et al. In vitro performance and principles of anti-siphoning devices. Acta Neurochir (Wien) 2014;156:2191–9.
[5] Freimann FB, Sprung C. Shunting with gravitational valves - can adjustments end the era of revisions for over drainage-related events? J Neurosurg 2012;117:1197–204.
[6] Lemcke J, Meier U, Muller C, et al. Safety and efficacy of gravitational shunt valves in patients with idiopathic normal pressure hydrocephalus: a pragmatic, randomized, open label, multicenter trial (SVASONA). J Neurol Neurosurg Psychiatry 2013;84: 850–7.
[7] Sprung C, Schlosser HG, Lemcke J, et al. The adjustable proGAV shunt: a prospective safety and reliability multicenter study. Neurosurgery 2010;66:465–74.
[8] Akbar M, Stippich C, Aschoff A. Letter to the editor: loss adjustability of Codman-Medos hydrocephalus valves after exposure to 3.0 T MRI. N Engl J Med 2005: 1413–4.
[9] Anderson RC, Walker ML, Viner JM, et al. Adjustment and malfunction of a programmable valve after exposure to toy magnets. Case report. J Neurosurg 2004;101: 222–5.
[10] Lavinio A, Harding S, Van Der Boogaard F, et al. Magnetic field interactions in adjustable hydrocephalus shunts. J Neurosurg Pediatr 2008;2:222–8.
[11] Nakashima K, Nakajo T, Kawamo M, et al. Programmable shunt valves: in vitro assessment of safety of the magnetic field generated by a portable game machine. Neurol Med Chir (Tokyo) 2011;51:635–8.
[12] Nakashima K, Oishi A, Itokawa H, et al. Effect of magnetic fields from home-use magnetic induction therapy apparatuses on adjustable cerebrospinal fluid shunt valves. No Shinkei Geka 2010;38:725–9.
[13] Schneider T, Knauff U, Nitsch J, et al. Electromagnetic field hazards involving adjustable shunt valves in hydrocephalus. J Neurosurg 2002;96:331–4.
[14] Zuzak TJ, Balmer B, Schmidig D, et al. Magnetic toys: forbidden for pediatric patients with certain programmable shunt valves? Childs Nerv Syst 2009;25:161–4.
[15] Lindner D, Preul C, Trantakis C, et al. Effect of 3 T MRI on the function of shunt valves—evaluation of Paedi GAV, dual switch and proGAV. Eur J Radiol 2005;56: 56–9.
[16] Toma AK, Tarnaris A, Grieve JP, et al. Adjustable shunt valve-induced magnetic resonance imaging artifact: a comparative study. J Neurosurg 2010;113:74–8.

[17] Shellock FG. Reference manual for magnetic resonance safety, implants, and devices: 2017 edition. Los Angeles, CA: Biomedical Research Publishing Group; 2017.
[18] Shellock FG, Bedwinek A, Oliver-Allen M, et al. Assessment of MRI issues for a 3-T "immune" programmable CSF shunt valve. AJR Am J Roentgenol 2011;197:202–7.
[19] Shellock FG, Habibi R, Knebel J. Programmable CSF shunt valve: in vitro assessment of MR imaging safety at 3 T. Am J Neuroradiol 2006;27:661–5.
[20] Shellock FG, Knebel J, Prat AD. Evaluation of MRI issues for a new neurological implant, the sensor reservoir. Magn Reson Imaging 2013;31:1245–50.
[21] American Society for Testing and Materials International. Designation F 2052–02: standard test method for measurement of magnetically induced displacement force on passive implants in the magnetic resonance environment. West Conshohocken, PA: ASTM International; 2002.
[22] Shellock FG, Kanal E, Gilk T. Confusion regarding the value reported for the term "spatial gradient magnetic field" and how this information is applied to labeling of medical implants and devices. AJR Am J Roentgenol 2011;196:142–5.
[23] American Society for Testing and Materials International. Designation F2182–11a standard test method for measurement of radio frequency induced heating on or near passive implants during magnetic resonance imaging. ASTM International; 2011.
[24] Weiland JD, Faraji B, Greenberg RJ, Humayun MS, Shellock FG. Assessment of MRI issues for the Argus II retinal prosthesis. Magn Reson Imaging 2012;30:382–9.
[25] Shellock FG, Woods TO, Crues JV. MRI labeling information for implants and devices: explanation of terminology. Radiology 2009;253:26–30.